ACS OMEGA

Open Access

http://pubs.acs.org/journal/acsodf

Article

Investigation of Filtration Performances in Eggshell Ultrafiltration Membranes with Surface Functionalized Using Graphene Oxide

Fitri Fitrilawati,* Gita Maulida, Ayi Bahtiar, Norman Syakir, and I Made Joni

Cite This: *ACS Omega* 2024, 9, 51052−51061

Read Online

ACCESS | Metrics & More | Article Recommendations

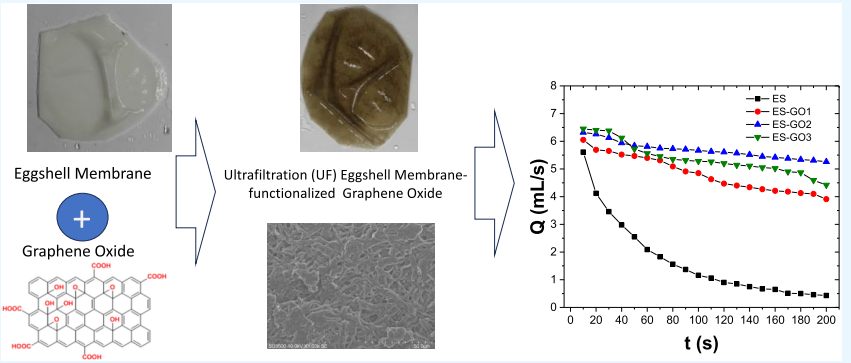

ABSTRACT: Efforts to prevent fouling are crucial in advancing ultrafiltration (UF) membranes, especially in addressing the concentration polarization of the accumulation of dissolved dye molecules in wastewater. This study explores the impact of incorporating graphene oxide (GO) onto eggshell (ES) UF membranes regarding their permeability, rejection efficiency, and permeate flow rate. The ES-GO membranes were obtained from eggshells that were modified with varied concentrations of GO (0.25, 0.5, and 0.75 mg/mL) through a self-assembly method. The performance of these ES-GO membranes was evaluated under different applied pressures (15, 30, 45, and 60 psi) to enhance the filtration capabilities. The assessment focused on membrane permeability, rejection efficiency, and permeate flow rate by measuring flow discharge. The results show that the addition of GO as a surface functionalization effectively prevents fouling and enhances the membrane's performance, achieving a membrane permeability of 2.854×10^{-3} Darcy and a stable filtration flow rate of approximately 5 mL/s. The most notable improvements in permeability and rejection efficiency were observed using ES-GO UF membranes with 0.5 mg/mL GO at a pressure of 45 psi, yielding a rejection efficiency of 36.6%, as seen in previous studies. Thus, the integration of GO into the ES membrane significantly reduces methylene blue (MB) concentration while maintaining a high flux rates, underscoring GO's role as an effective cohost for minimizing fouling in the filtration process.

INTRODUCTION

Water is a critical resource for human activities, including those in industries, such as textiles. The production processes in the textile industry, particularly dyeing, significantly impact water quality due to the release of wastewater with synthetic dyes that are resistant to degradation. When these dyes, which are often present in high concentrations, are discharged untreated into the environment, they will contribute to severe water pollution. Traditional wastewater treatment methods for dye removal can be classified into three main categories: physical (e.g., centrifugal separation, adsorption),[1−6] chemical (e.g., coagulation, electrolysis, and oxidation),[7−14] and biological (e.g., anaerobic and aerobic processes).[15−17] However, these conventional methods often suffer from drawbacks, such as high operational costs, the generation of secondary pollutants, and the production of harmful by products and large volumes of sludge. Particularly challenging are dyes like methylene blue (MB), which is nonbiodegradable due to its benzene ring structure, making it difficult to break down. Addressing the issue of clean water contaminated by synthetic dyes requires innovative, cost-effective, and environmentally friendly purification technologies. Many approaches have been developed to purify color polluted water, such as photocatalytic degradation processes,[18] adsorption,[19] and membrane filtration.[20] Among various approaches, membrane-based separation techniques, including microfiltration (MF), nanofiltration (NF), reverse

Received: June 24, 2024
Revised: November 13, 2024
Accepted: November 25, 2024
Published: December 16, 2024

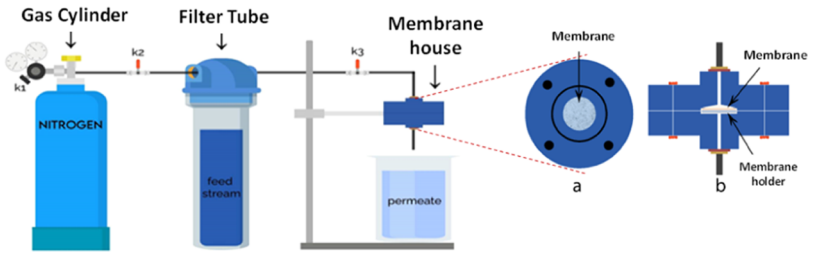

Figure 1. Filtration apparatus consists of a nitrogen gas cylinder, a filter tube, a k1 valve, a k2 valve, a filter tube, a k3 valve, the membrane housing, and permeate container.

osmosis (RO), and membrane distillation (MD), have emerged as promising solutions for treating dyeing wastewater and improving water quality.

Graphene oxide (GO) has gained considerable attention as a promising membrane material.[21−23] A two-dimensional structure allows the incorporation of GO into the surfaces, allowing the use of lower pressures compared to polymeric nanofiltration membranes.[24] The nanochannels formed during the membrane production of GO enable ultrafast water transport through the membranes.[25] Furthermore, the construction of GO membranes with photocatalytic self-cleaning[26] and ion sorption in GO membranes[27] has been reported to be ideal for water filtration membranes. The adsorption process is a commonly employed technique for purifying water contaminated with dyes. Zhang et al. demonstrated that GO is highly effective in removing MB through adsorption.[28] Previous studies have confirmed that GO exhibits significant adsorption efficiency for MB molecules in aqueous solutions.[29,30] The effectiveness of GO in this role is attributed to its oxygen-containing functional groups—such as hydroxyl, carboxyl, carbonyl, and epoxide—which enhance its hydrophilicity and facilitate its dispersion in water.[28] Furthermore, GO's large surface-to-volume ratio (STV) contributes to its superior adsorption capabilities. Despite these advantages, the static nature of the adsorption process limits its efficiency as additional steps are needed to separate the adsorbent from the treated water. Therefore, a more direct method for producing clean water, such as filtration, is preferable. Filtration offers a straightforward approach, where contaminated water passes through a membrane to yield purified water directly. Combining adsorption with filtration could potentially enhance the overall performance.

Recent research has explored various membrane materials for water purification, including biomaterials such as eggshell (ES) membranes. The ES membrane, which consists of semipermeable protein fibers, is insoluble in water and features a substantial surface area. Its functional groups, such as hydroxyl, thiol, carboxyl, amino, and amide, make it an effective adsorbent for removing a range of organic and inorganic contaminants from wastewater.[28] Notably, studies have shown that graphene oxide-modified eggshell membranes (ES-GO) are highly effective in adsorbing fluoride ions.[31] Zhang et al. have also investigated the use of ES membranes combined with GO and gold nanoparticles (AuNPs) for harvesting sunlight-driven photothermal effects.[32] Additionally, eco-friendly ES membranes have been functionalized with various materials for diverse applications, including solid-phase extraction of lead ions (Pb II),[33] visible light-induced antibacterial activity against *Escherichia coli*,[34] and the development of biotriboelectric nanogenerators and smart sensors.[35]

In our previous research, we explored the use of eco-friendly ES membranes integrated with GO adsorbents for the filtration of MB from wastewater. Our findings demonstrated that ES-GO membranes were highly effective in reducing MB concentrations during the filtration process.[36] Despite these promising results, there is limited research addressing the impact of membrane surface functionalization on the prevention of fouling due to concentration polarization. This phenomenon causes dissolved molecules to accumulate at the membrane surface, while nondissolved materials can either adhere directly to the membrane or deposit on existing.

In this study, we expand on this by investigating the permeability, rejection efficiency, and permeate flow rate of ultrafiltration (UF) ES membranes modified with varying concentrations of GO. Our aim is to enhance membrane performance in removing MB from wastewater through filtration. MB, which is a synthetic dye commonly used in the textile industry, was selected as the target contaminant. Additionally, we assessed the role of GO as a cohost adsorbent in improving the filtration efficiency of the ES membranes in removing MB molecules. The novelty of the present study showed that the incorporation of GO into the ES membrane significantly enhanced the filtration performance compared to the unmodified ES membrane while also maintaining a high flux rate.

MATERIALS AND METHODS

Materials. Fresh hen eggs were purchased from a local market. To obtain the ES membranes, acetic acid (Merck) was used to dissolve the outer ES layer. The ethanol (Merck) was used to keep the ES membrane. GO dispersion in water with a concentration of 4 mg/mL was purchased from Graphenea (GO, Graphenea SA ES A75022608). The milli-Q water that was used to dilute the GO dispersion was obtained from Millipore (18 MΩ/cm). MB was used as a pollutant model that was purchased from Merck (C.I. 52015 Merck). The MB solution was prepared by using distilled water.

Methods. *Preparation and Characterization of ES-GO Composite Membranes.* The ES membranes were obtained by manually detaching the inner layer of chicken eggshells from the outer shell using a 15% acetic acid solution. After a 30 min immersion, the ES membranes were separated from the outer shell and removed from the acetic acid. They were then thoroughly rinsed with distilled water. To prevent drying, the membranes were stored in a sealed glass container with ethanol prior to modification. For the preparation of ES-GO membranes, the ES membrane surfaces were enhanced using GO dispersion, as described in previous studies.[36] The GO dispersion (0.5 mg/mL) was prepared by diluting 2.5 mL of a 4 mg/mL GO solution with 17.5 mL of Milli-Q water. Prior to modification, the GO dispersion was stirred at 250 rpm for 15

https://doi.org/10.1021/acsomega.4c05853
ACS Omega 2024, 9, 51052−51061

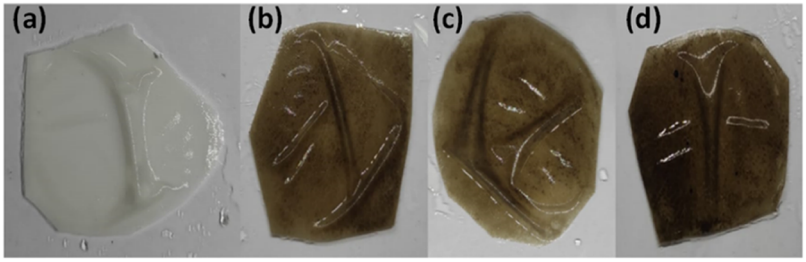

Figure 2. Comparison of ES membrane and ES membrane modified GO (a) ES membrane, (b) ES-GO1 membrane, (c) ES-GO2 membrane, and (d) ES-GO3 membrane.

min and then sonicated in an ultrasonic bath (Branson 1800) at room temperature for 30 min. The ES membranes were rinsed with distilled water and dried before being immersed in the GO dispersion and placed in the ultrasonic bath for 3 h. After modification, the ES-GO membranes were rinsed with distilled water and dried. The ES-GO membranes were prepared using GO dispersions with concentrations of 0.25, 0.5, and 0.75 mg/mL. The morphology and molecular structure of the ES and ES-GO membranes were measured using scanning electron microscopy (SEM, Hitachi SU-3500) and Fourier transform infrared spectroscopy (FTIR, Thermo Scientific Nicolet iS5). Furthermore, from the SEM images, we estimated the diameter of membrane pore using imageJ software.

Filtration of Methylene Blue Using ES-GO membranes. A 5 ppm (5 mg/L) MB solution was used as the pollutant model. The GO-modified ES membrane served as the filtration membrane in the experiments. Filtration tests were conducted using a filtration setup, illustrated in Figure 1, based on the configuration from ref 36. This apparatus includes a nitrogen gas cylinder to regulate pressure, a k1 valve to maintain pressure within the cylinder, and a k2 valve to control pressure flow into the filter tube. The filter tube acts as a reservoir for the MB solution, while the k3 valve prevents the solution from exiting the filter tube and entering the membrane housing. The membrane housing contains the membrane during filtration and the glass beaker for collecting the permeate postfiltration. When the pressure was applied, the MB solution was pushed through the membrane. Upon opening the k3 valve, the MB solution filtered through the membrane, and the permeate was collected in a glass beaker. The volume of collected permeate was recorded over time. Changes in permeate concentration were monitored by measuring absorbance using a UV−vis spectrophotometer (Edinburgh Instrument DS5) within the wavelength range of 500−750 nm.

The filtration experiment commenced with the membrane being secured in the membrane holder and the membrane positioned within the apparatus. A 1000 mL reservoir tube was then filled with a 5 ppm of MB solution. The first valve was opened, and nitrogen pressure was adjusted to the desired level. Subsequently, the second valve was opened to allow pressure to flow into the reservoir tube, pushing the MB solution toward the membrane and initiating the filtration process. The third valve was then opened to let the filtered MB solution (permeate) exit and collect in a beaker. The volume of the permeate (VP) was measured at various filtration intervals. Both the MB solution and the collected permeate were measured at different time points using a UV−vis spectrophotometer in the 500−750 nm range. The concentration of MB permeate was determined by using a calibration curve. Additionally, experiments were conducted with varying pressures (15, 30, 45, and 60 psi) and using ES-GO membranes with different GO concentrations to assess their impact on the filtration performance.

Permeability and Rejection Efficiency of ES-GO UF Membranes. The permeability of the membrane was determined from experimental data on flow discharge for UF membranes with varying surface areas and GO concentrations under a pressure difference of 45 psi (3.062 atm), fluid viscosity of 0.97 Ns m^{-2} (970 cP), and membrane thickness of 0.007 cm (70 μm). Permeability reflects the volume of fluid passing through the membrane, with higher permeability indicating a substantial increase in flow discharge, while lower permeability signifies a minimal change. This parameter is influenced by factors, such as pore density, pore size, operating pressure, and membrane thickness. To estimate the membrane permeability (κ), the flow discharge values collected during filtration tests were used. Permeability was calculated using Darcy's law (eq 1), incorporating parameters such as the permeate flow rate Q (in L h^{-1}), membrane permeability κ (in $L{\cdot}m^{-2}{\cdot}h^{-1}{\cdot}bar^{-1}$), membrane area A (in m^2), membrane thickness L (in m), permeate viscosity μ (in Pa s), and applied pressure ΔP (in Pa).[37] For cgs units, Q is expressed in cm^3 s^{-1}, κ in Darcy, A in cm^2, μ in cP, and ΔP in atm.

$$Q = \kappa\left(\frac{A}{\mu L}\right)\Delta P \tag{1}$$

$$\kappa = \left(\frac{\mu L}{A}\right)\left(\frac{Q}{\Delta P}\right) \tag{2}$$

$$R = \left(\frac{c_o - c_n}{c_o}\right) \times 100\% \tag{3}$$

The rejection coefficient measures a membrane's effectiveness in retaining or allowing the passage of particles or dissolved molecules and can be calculated using eq 3, where R represents the rejection coefficient (%), C_o is the initial concentration of MB (mg/L), and C_n is the final concentration of MB (mg/L). The concentration of MB permeate was evaluate from absorbance of MB permeate at specific wavelengths using the calibration curve. The rejection coefficient indicates the proportion of MB molecules retained by the membrane. A lower rejection coefficient implies that the membrane allows more molecules to pass through, while a higher rejection coefficient suggests that the membrane is more effective at filtering out pollutant molecules.

https://doi.org/10.1021/acsomega.4c05853
ACS Omega 2024, 9, 51052−51061

RESULTS AND DISCUSSION

ES-GO Membranes. Figure 2 displays images of the ES-GO membranes in comparison with the plain ES membrane. The ES membrane retains its original white appearance (Figure 2a), whereas the ES-GO membranes exhibit a darker hue due to the presence of GO flakes decorating their surfaces (Figure 2b,c). The color change in the ES membranes after modification with GO signifies the formation of the ES-GO membrane. The GO does not wash away when thoroughly rinsed with distilled water; it seems that GO was embedded in the ES surface. It was reported that the interaction between GO and ES showed the increment of hydroxyl (O−H) and carboxyl (C−O) functional groups as increasing in ES amount.[38] The ES-GO membranes treated with a GO dispersion at a concentration of 0.25 mg/mL (ES-GO1) show a relatively uniform surface appearance (Figure 2b), though some areas still have noticeable spots, indicating incomplete coverage of the GO layer. In contrast, the ES membrane modified with a 0.5 mg/mL GO dispersion (ES-GO2) (Figure 2c) demonstrates a more even distribution of GO with fewer surface spots. Figure 2d illustrates the ES membrane treated with a higher concentration of GO dispersion (0.75 mg/mL, ES-GO3), which appears significantly darker, reflecting more extensive GO coverage on the ES membrane surface.

Filtration of MB Solution in ES-GO UF Membranes. Three types of GO-modified ES membranes were used in this experiment, i.e., ES-GO1, ES-GO2, and ES-GO3, prepared with GO dispersions of 0.25, 0.5, and 0.75 mg/mL, respectively. The filtration characteristics of these membranes, including permeate flux and concentration changes, are illustrated in Figure 3. The figure presents the variation of permeate flux (Q) over time (t) of different types of ES membranes. The results show that all UF membranes effectively allow water to flow while filtering dissolved MB. Over time, the ES membrane exhibits a decrease in flux discharge, eventually halting after a few minutes due to pore fouling caused by MB adsorption. In contrast, the GO-enhanced surface ES membrane (ES-GO) demonstrated improved flux discharge. The ES-GO1 membrane, that modified with 0.25 mg/mL GO dispersion, shows a slight reduction in flux from 6 to 5.5 mL/s in the first 60 min, decreasing further to 4 mL/s after 200 min. The ES-GO2 membrane maintains a relatively high discharge rate of about 5 mL/s after 200 min, while the ES-GO3 membrane exhibits a marginally lower flux than ES-GO2, as depicted in Figure 3a. Overall, the ES-GO membranes demonstrate higher flux compared to the unmodified ES membrane, which, as reported in previous studies, experienced significant fouling leading to a rapid decrease in discharge and premature termination of filtration.[36] The modification of the ES membrane with GO effectively prevents fouling, enhancing the performance of the UF membranes.

The filtration results for the ES and ES-GO membranes indicate a decrease in the MB concentration, as shown in Figure 3b. The MB concentration was determined using a calibration curve based on the absorbance of the filtered permeate at 664 nm. Initially, the MB concentration in the permeate from the ES membrane dropped sharply by about 40% from the starting concentration of 5 mg/L. However, as filtration continued, the concentration in the permeate increased, likely due to rewashing of the membrane, which

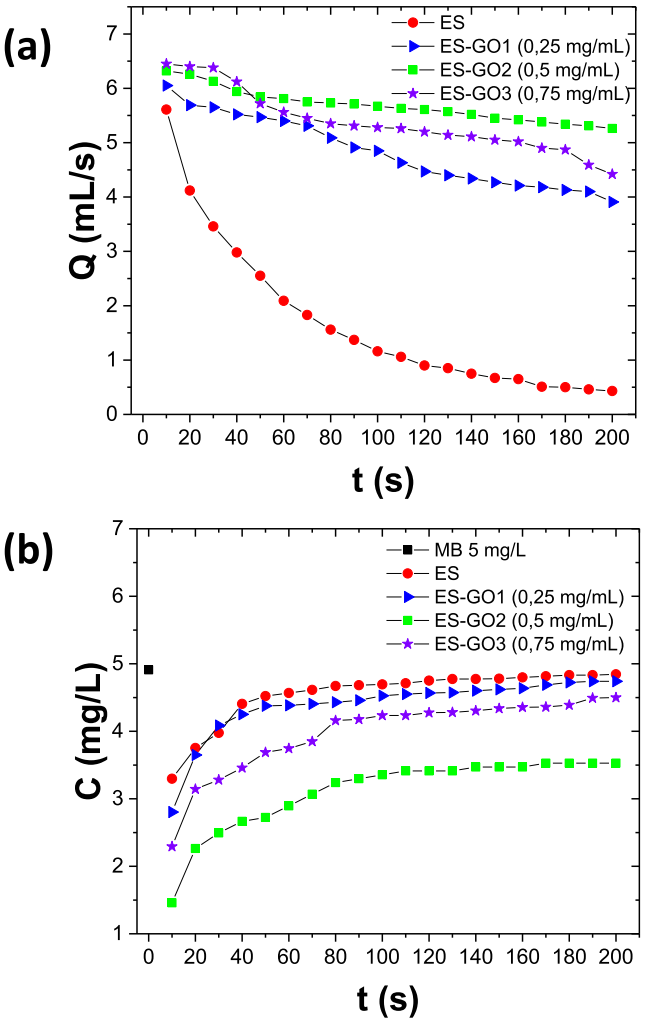

Figure 3. (a) Filtration flow discharge of MB solution through ES and ES-GO membranes. (b) Change of MB concentration of permeate as a result of filtration using ES and ES-GO membranes.

allowed previously absorbed MB molecules to re-enter the permeate. The ES-GO membranes displayed a similar trend in permeate concentration.

Incorporating GO into the ES membranes (ES-GO1, ES-GO2, and ES-GO3) effectively reduced the permeate concentration of MB. Among them, the ES-GO2 membrane showed the most significant reduction in MB concentration and achieved greater stability in permeate concentration compared to other membranes. The ES-GO2 membrane was identified as the most effective for MB filtration due to its ability to lower the MB concentration, maintain high flow discharge, and reach filtration stability more quickly. This indicates that GO modification substantially improves the filtration performance compared with the unmodified ES membrane.

Furthermore, the filtration process was evaluated at varying pressures of 15 psi (1.021 atm), 30 psi (2.041 atm), 45 psi (3.062 atm), and 60 psi (4.083 atm) to evaluate their impact on flow discharge and permeate concentration. Figure 4a shows the flow discharge of the ES-GO2 membrane at different pressures. The graph illustrates that while the ES-GO2 membrane facilitates MB solution passage, the flow discharge decreases over time, likely due to MB accumulation on the membrane surface disrupting the flow. At 45 psi, the ES-GO2

https://doi.org/10.1021/acsomega.4c05853
ACS Omega 2024, 9, 51052−51061

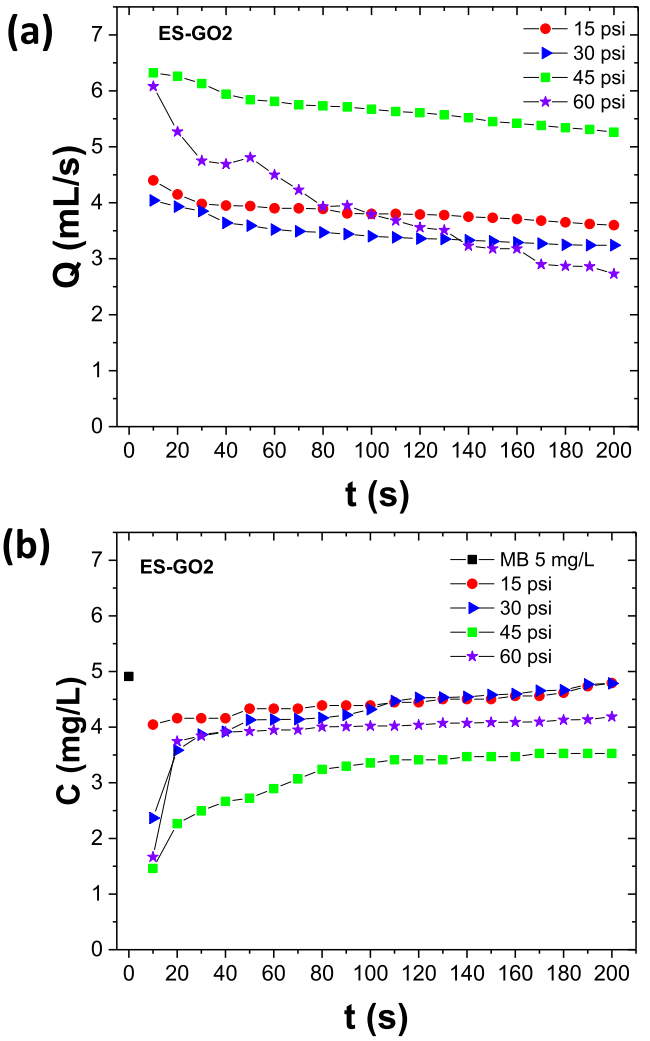

Figure 4. (a) Flow discharge and (b) change of concentration of filtrate using the ES-GO2 membrane at varied pressures.

membrane maintains a relatively constant flow rate of 5 mL/s, which is higher compared with other pressures. After 120 s, the flow rate only slightly diminishes, suggesting that MB molecules might be partially blocking the membrane pores.

Figure 4b presents a graph showing the relationship between permeate concentration measured every 10 s and the sampling time for each pressure variation. On the vertical axis, C represents the filtrate concentration of the permeate, while the horizontal axis, *t*, denotes the filtration sampling time. The data reveal that the permeate concentration at all four pressure settings initially dropped compared to the starting MB concentration of 5 mg/L. However, as the sampling time increased, the permeate concentration rose again relative to the first filtration results.

The results indicate that the permeate concentration remained lower than the initial MB concentration, demonstrating that the ES-GO2 membrane effectively filtered the MB molecules. This suggests that the pressure influences the filtration process by impacting the MB concentration reduction. A decrease in the MB concentration implies adsorption of MB by the ES and GO membranes; without adsorption, no reduction in MB concentration would occur. Among the four pressure variations tested, 45 psi (3.062 atm) proved to be the most effective in reducing the MB concentration. At this pressure, the MB concentration decreased by nearly 70% during the initial filtration, and the final permeate concentration was significantly lower than that observed at pressures of 15, 30, and 60 psi.

Permeability and Rejection Efficiency of ES-GO UF Membranes. To evaluate the impact of GO on the performance of the ES membrane, Figure 5 illustrates the

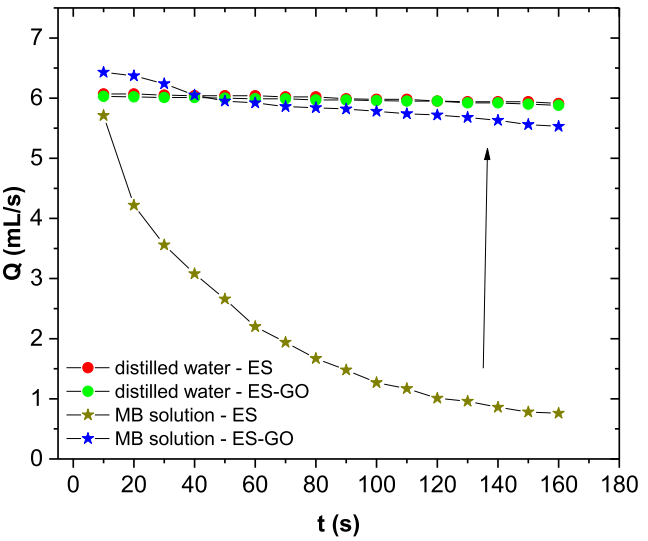

Figure 5. Filtration flow discharge of distilled water and MB solution through ES and ES-GO-2 membranes at a pressure of 45 psi.

filtration flow discharge for both distilled water and the MB solution through the ES and ES-GO membranes. The results show that the type of test solution significantly affects the flow discharge. For distilled water, the flow discharge through both the ES and ES-GO membranes remained relatively stable. This is expected, as distilled water is pure and does not interact with the membrane material. However, when the ES membrane was used to filter the MB solution, the flow discharge dropped rapidly, leading to a cessation of the filtration process. This decline is likely due to fouling caused by pore blockage, as the ES membrane's hydroxyl groups (O−H) may interact with MB molecules, leading to their accumulation and constriction of the pores.

In contrast, Figure 5 shows that the flow discharge for the MB solution through the ES-GO membrane remained relatively stable, with only a slight decrease. This indicates minimal fouling, as the ES-GO membrane was able to maintain a high flow rate throughout the filtration process. The presence of GO appears to reduce fouling by covering the membrane fibers, preventing MB molecules from binding and causing blockages. Thus, the incorporation of GO into the ES membrane enhances its performance in filtering MB solutions by reducing fouling and maintaining consistent flow discharge

Figure 6a illustrates the changes in the membrane permeability over time for ES membranes modified with different GO concentrations. The ES membrane without modification exhibits a significant drop in permeability from initial to final stages due to rapid fouling and resulting decreases in flow discharge, leading to an abrupt end of the filtration process. In contrast, the ES-GO membranes show only a minor difference between initial and final permeability values, with the ES-GO2 membrane maintaining the highest flow discharge. This minimal change in permeability indicates

https://doi.org/10.1021/acsomega.4c05853
ACS Omega 2024, 9, 51052−51061

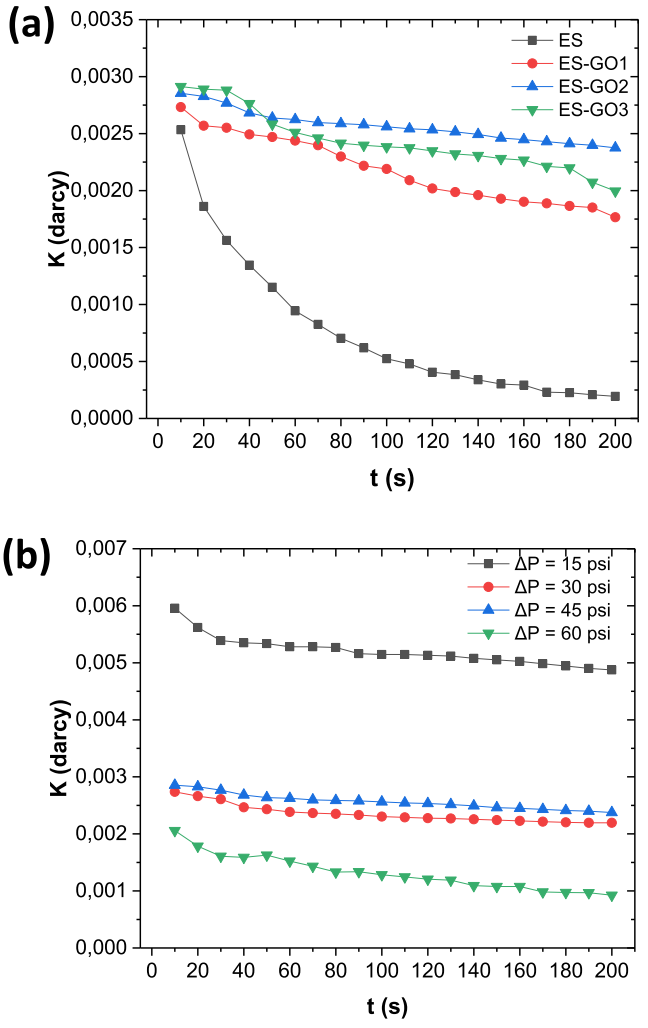

Figure 6. Membrane permeability of filtration results using the GO-modified ES membrane with (a) varied GO concentration and (b) pressure variation.

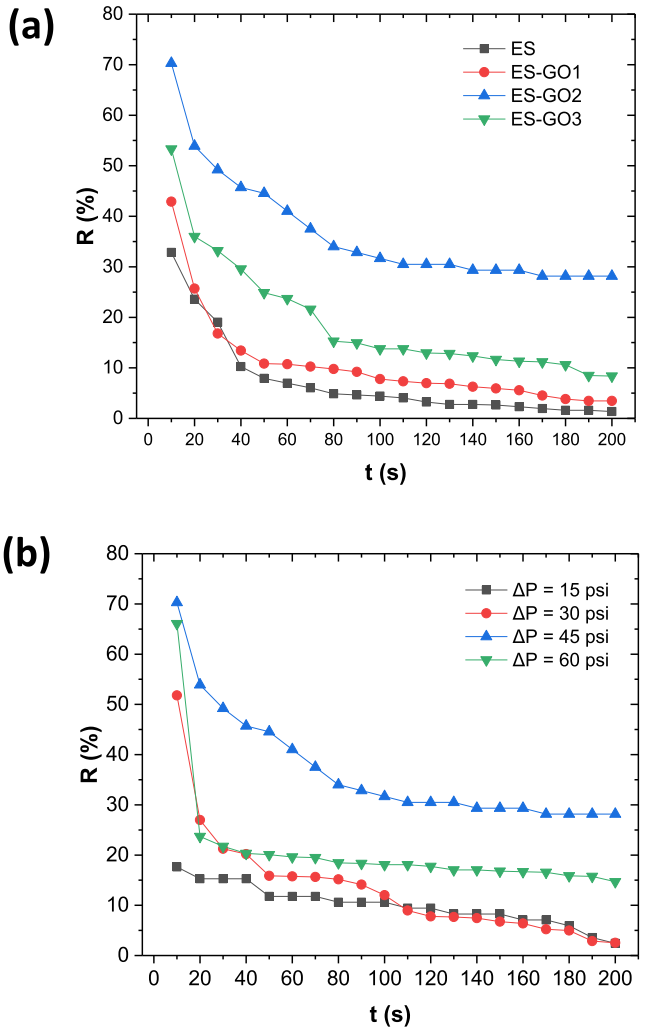

Figure 7. Rejection coefficient of filtration results using ES-GO membranes with (a) varied GO concentration 45 psi and (b) using ES-GO2 with varied pressure.

that the ES-GO membranes sustain substantial flow discharge throughout the filtration process.

Figure 6b depicts the membrane permeability changes as a function of time under different pressure settings. At a pressure of 45 psi, the minimal difference between initial and final permeability suggests that the flow discharge remains relatively high compared to those at other pressures.

Figure 7a presents the variation in the rejection coefficient over time for ES-GO membranes with different GO concentrations. The data reveal that GO incorporation enhances the membrane's ability to reject MB molecules, with the ES-GO2 membrane showing the highest rejection coefficient among the ES-GO1 and ES-GO3 membranes. Initially, the ES-GO2 membrane achieves a rejection rate of approximately 70%, decreasing to around 30% after 200 min. Figure 7b shows the change in the rejection coefficient over time with varying pressures. The results indicate that higher pressure improves the membrane's rejection capability, with 45 psi yielding the highest rejection coefficient around 70% initially and approximately 30% by the end of filtration.

Unlike the ES membrane, in which water flows through the pores of the membrane, in the ES-GO composite membrane, the mass transfer channels are performed by the stacking of GO nanosheets. Thus, interconnected nanochannels between the adjacent nanosheets of a few-layered GO-gated membranes offer great opportunities for ultrafast molecular-separation membranes.[39,40] In addition, GO has a practically frictionless surface, water flow through these nanochannels more quickly, and this can be considered the main advantage of using GO to modify or manufacture membranes.[41,42] Furthermore, these nanochannels are responsible for the size exclusion mechanism; while water molecules pass through the membrane, the molecules that are larger than the channel might be retained. Also, the oxygen-containing functional groups interact electrostatically with ions present in the solution to be filtrated, thus enhancing the selective permeation of the ions through the membrane.[43,44]

Characteristics and Filtration Mechanism of ES-GO UF Membranes. The primary filtration mechanisms for microfiltration (MF) and ultrafiltration (UF) are based on the sieving principle, where molecules larger than the membrane pores are rejected. Both processes employ porous membranes, making pore flow a relevant consideration, particularly for UF membranes where fouling and concentration polarization on the membrane's feed side can significantly impact performance.

Figure 8 displays the infrared spectra of the ES membrane and the modified ES-GO membranes with various GO

https://doi.org/10.1021/acsomega.4c05853
ACS Omega 2024, 9, 51052−51061

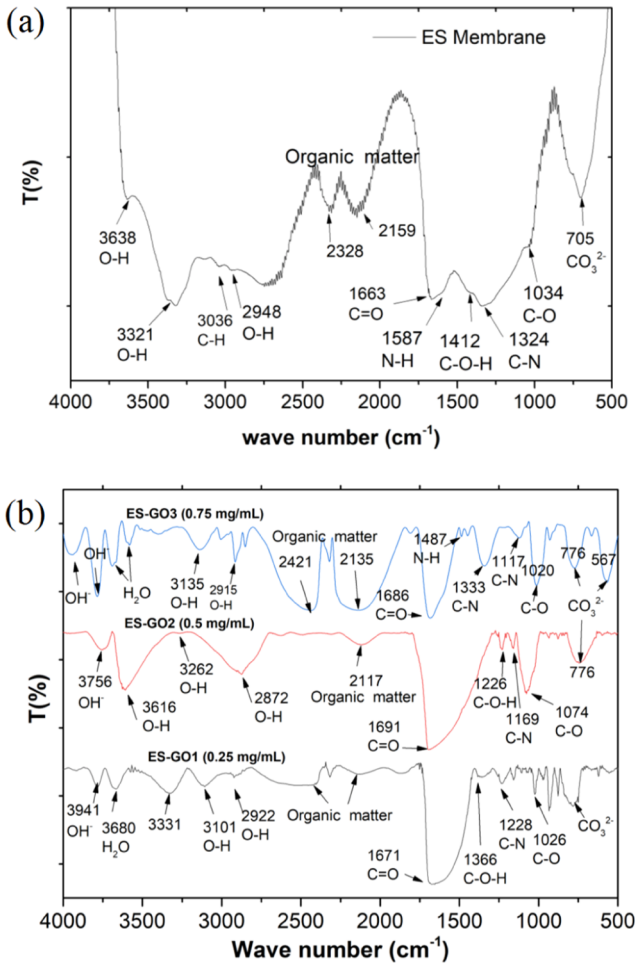

Figure 8. (a) Infrared spectrum of ES membrane and (b) infrared spectra of ES-GO membrane modified with a varied concentration of GO dispersion.

concentrations. The ES membrane spectrum in Figure 8a reveals a matrix of glycoproteins, uronic acid, sialic acid, and various amino acids. Further analysis of the IR spectrum revealed CO_3^{2-} substitution, as identified by characteristic peaks of CO_3^{2-} at around 700 cm^{-1}, which are attributed to the vibrational modes of the carbonate ions substituted at the hydroxide ion (A-type).[45] Two peaks appeared at 2328 and 2159 cm^{-1} assigned to the organic matter of the ES membrane. Notable peaks include 1587 cm^{-1}, corresponding to N−H stretching (amide A), and 3036 cm^{-1}, indicating C−H asymmetry. The peak at 1663 cm^{-1} is attributed to C═O stretching in amide I (glycoprotein), while other characteristic peaks at 1034 cm^{-1} (C−O), 3638 and 2948 cm^{-1} (O−H), and 1412 cm^{-1} (C−O−H) further define the ES membrane. These findings confirm the presence of peptide bonds and various functional groups characteristic of the ES membrane.

In contrast, Figure 8b presents the spectra of ES membranes modified with a GO dispersion. The analysis showed that characteristic peaks of CO_3^{2-} remained in the ES-GO membranes. In contrast, ES-GO spectra had bands corresponding to (−OH) and H_2O at 3500−4000 cm^{-1}[45] Two peaks for organic matter remain appeared in ES-GO1 and ES-GO3 with lower intensity compared with ES. In contrast, the peaks for organic matter reduced significantly indicating successful functionality of GO into ES membrane. Remain within the same spectral groups, and there are noticeable shifts in the wavelengths, indicating successful surface modification by GO. These wavelength shifts suggest physical interactions between the ES membrane and GO flakes, resulting in changes in the spectral characteristics. The ES membrane, an extracellular matrix, is known to be produced in the tubular glands of the white isthmus and then secreted into the oviduct, where it assembles into a reticular structure.[46,47] The specific proteins involved in eggshell membrane formation have been well-documented.[48] This membrane's unique physical structure is characterized by disulfide bonds and cross-linking between protein molecules and lysine-derived chains.

The observed reduction in permeability may be attributed to concentration polarization, a common phenomenon in membrane filtration where particles or solutes accumulate in a boundary layer near the membrane surface, decreasing the solvent activity and flow. As demonstrated in Figures 5 and 6, this accumulation leads to a decrease in solvent flux through the membrane due to reduced effective trans-membrane pressure (TMP), caused by osmotic pressure differences between the filtrate and feed solution. Although concentration polarization is an inherent limitation, it is reversible by adjusting the TMP. Additionally, the interaction between MB and the UF membrane involves electrostatic or ionic forces between the positively charged MB molecules and the negatively charged −OH groups on the GO surfaces as well as interactions with oxygen-containing groups such as carboxyl (−COOH), epoxy (C−O), and hydroxyl (−OH) on GO sheets. These functional groups act as active sites for MB adsorption.

Figure 9 illustrates the surface morphology of the ES membrane before and after modification with GO, as observed by SEM, along with the corresponding surface pore size distributions. Prior to GO modification, Figure 9a shows that the ES membrane consists of fibrous structures that interconnect to form a porous layer with visible voids. After modification, Figure 9b depicts the surface of the ES-GO1 membrane. The fibers on the ES-GO1 membrane appear rougher compared to the untreated ES membrane, indicating surface changes due to GO deposition. In Figure 9c, the ES-GO2 membrane shows fibers adorned with GO flakes and retains some voids, suggesting the formation of a composite material. However, the ES-GO3 membrane, with a higher GO concentration (0.75 mg/mL), exhibits irregular fiber morphology as seen in Figure 9d. This irregularity may be attributed to excessive GO concentration, leading to uneven distribution on the ES membrane surface.

The pore size distribution in Figure 9b−d reveals that some voids in the ES-GO membranes are covered by GO flakes. In contrast, the ES-GO2 (Figure 9c) likely had a pore size distribution that was more homogeneous compared to the other treated ES membrane. This reduction in pore size distribution after GO treatment signifies the successful formation of ES-GO composites. Smaller pore sizes in the ES-GO membranes can enhance filtration efficiency by enabling the retention of smaller particles or molecules. In prior studies, achieving similar filtration capabilities required three layers of ES membrane.[49]

Through GO in the membrane surfaces, the oxygen-containing functional groups interact electrostatically with ions in the dye molecules, thus enhancing the antifouling effect.[50,51] The decrease in the surface of the membrane and an

https://doi.org/10.1021/acsomega.4c05853
ACS Omega 2024, 9, 51052−51061

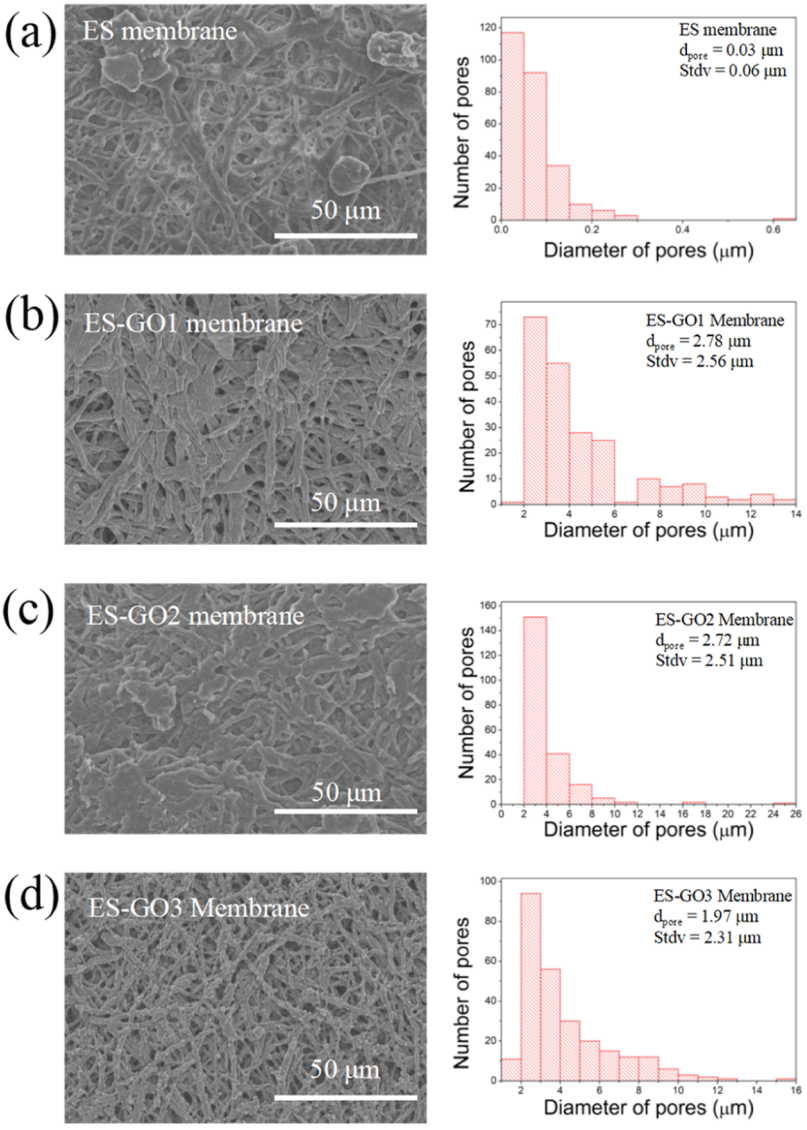

Figure 9. Comparison of ES membrane surface morphology and ES membrane modified with GO (a) ES membrane, (b) ES-GO1 membrane (0.25 mg/mL), (c) ES-GO2 membrane (0.5 mg/mL), and (d) ES-GO3 membrane (0.75 mg/mL).

increase in membrane hydrophilicity contribute to the modified membrane against fouling.[52]

CONCLUSIONS

In summary, the incorporation of GO into the ES membrane significantly enhanced the filtration performance compared to the unmodified ES membrane while also maintaining a high flux rate. The presence of GO on the membrane surface effectively prevents fouling, related to its role in modifying pore surfaces and improving their functional characteristics. Among the tested configurations, the UF ES membranes modified with 0.5 mg/mL GO exhibited the best performance. At a pressure of 45 psi, these membranes achieved the highest permeability and rejection rates, with an optimal rejection efficiency of 36.6% and a membrane permeability of 2.854×10^{-3} Darcy. Additionally, the filtration flow rate remained relatively stable, at approximately 5 mL/s. This demonstrates that GO surface functionalization not only prevents fouling but also optimizes both the filtration efficiency and operational stability.

AUTHOR INFORMATION

Corresponding Author

Fitri Fitrilawati − *Department of Physics, Faculty of Mathematics and Natural Science, Universitas Padjadjaran, Sumedang 45363, Indonesia; Functional Nano Powder University Centre of Excellence (FiNder UCoE), Universitas Padjadjaran, Sumedang 45363, Indonesia;* orcid.org/0000-0002-4255-6053; Email: fitrilawati@unpad.ac.id

Authors

Gita Maulida − *Department of Physics, Faculty of Mathematics and Natural Science, Universitas Padjadjaran, Sumedang 45363, Indonesia*

Ayi Bahtiar − *Department of Physics, Faculty of Mathematics and Natural Science, Universitas Padjadjaran, Sumedang 45363, Indonesia; Functional Nano Powder University Centre of Excellence (FiNder UCoE), Universitas Padjadjaran, Sumedang 45363, Indonesia*

Norman Syakir − *Department of Physics, Faculty of Mathematics and Natural Science, Universitas Padjadjaran, Sumedang 45363, Indonesia; Functional Nano Powder*

https://doi.org/10.1021/acsomega.4c05853
ACS Omega 2024, 9, 51052−51061

University Centre of Excellence (FiNder UCoE), Universitas Padjadjaran, Sumedang 45363, Indonesia

I Made Joni − *Department of Physics, Faculty of Mathematics and Natural Science, Universitas Padjadjaran, Sumedang 45363, Indonesia; Functional Nano Powder University Centre of Excellence (FiNder UCoE), Universitas Padjadjaran, Sumedang 45363, Indonesia;* orcid.org/0000-0001-5949-3418

Complete contact information is available at: https://pubs.acs.org/10.1021/acsomega.4c05853

Author Contributions

The manuscript was written through contributions of all authors. All authors have given approval to the final version of the manuscript.

Notes

The authors declare no competing financial interest.

■ ACKNOWLEDGMENTS

This work was funded by the Project Penelitian Dasar Unggulan Perguruan Tinggi (PDUPT) Contract Number 2064/UN6.3.1/PT.00/2022 dated 17th March 2022 and the ALG Project Universitas Padjadjaran Contract Number 1549/UN6.3.1/PT.00/2023 dated 27th March 2023.

■ REFERENCES

(1) Gupta, V. K.; Ali, I.; Saini, V. K. Adsorption studies on the removal of Vertigo Blue 49 and Orange DNA13 from aqueous solutions using carbon slurry developed from a waste material. *J. Colloid Interface Sci.* **2007**, *315*, 87−93.

(2) Hadi, P.; Guo, J.; Barford, J.; McKay, G. Multilayer dye adsorption in activated carbons-facile approach to exploit vacant sites and interlayer charge interaction. *Environ. Sci. Technol.* **2016**, *50*, 5041−5049.

(3) Nayak, S.; Prasad, S. R.; Mandal, D.; Das, P. Carbon dot cross-linked polyvinylpyrrolidone hybrid hydrogel for simultaneous dye adsorption, photodegradation and bacterial elimination from waste water. *J. Hazard. Mater.* **2020**, *392*, No. 122287.

(4) Wang, X.; Zhu, N.; Yin, B. Preparation of sludge-based activated carbon and its application in dye wastewater treatment. *J. Hazard. Mater.* **2008**, *153*, 22−27.

(5) Malik, P. K. Dye removal from wastewater using activated carbon developed from sawdust: adsorption equilibrium and kinetics. *J. Hazard. Mater.* **2004**, *113*, 81−88.

(6) Demirbas, A. Agricultural based activated carbons for the removal of dyes from aqueous solutions: a review. *J. Hazard. Mater.* **2009**, *167*, 1−9.

(7) Szpyrkowicz, L.; Juzzolino, C.; Kaul, S. N.; Daniele, S.; de Faveri, M. D. Electrochemical oxidation of dyeing baths bearing disperse dyes. *Ind. Eng. Chem. Res.* **2000**, *39*, 3241−3248.

(8) Ricordel, C.; Darchen, A.; Hadjiev, D. Electrocoagulation-electroflotation as a surface water treatment for industrial uses. *Separ. Purif. Technol.* **2010**, *74*, 342−347.

(9) Deka, B. J.; Jeong, S.; Tabatabai, S. A. A.; An, A. K. Mitigation of algal organic matter released from Chaetoceros affinis and Hymenomonas by in situ generated ferrate. *Chemosphere* **2018**, *206*, 718−726.

(10) Bae, W.; Won, H.; Hwang, B.; de Toledo, R. A.; Chung, J.; Kwon, K.; Shim, H. Characterization of refractory matters in dyeing wastewater during a full-scale Fenton process following pure-oxygen activated sludge treatment. *J. Hazard. Mater.* **2015**, *287*, 421−428.

(11) Wu, H.; Wang, S. Impacts of operating parameters on oxidation-reduction potential and pretreatment efficacy in the pretreatment of printing and dyeing wastewater by Fenton process. *J. Hazard. Mater.* **2012**, *243*, 86−94.

(12) Aravind, P.; Selvaraj, H.; Ferro, S.; Sundaram, M. An integrated (electro- and biooxidation) approach for remediation of industrial wastewater containing azo-dyes: understanding the degradation mechanism and toxicity assessment. *J. Hazard. Mater.* **2016**, *318*, 203−215.

(13) Zhu, X.; Ni, J.; Wei, J.; Xing, X.; Li, H. Destination of organic pollutants during electrochemical oxidation of biologically-pretreated dye wastewater using boron-doped diamond anode. *J. Hazard. Mater.* **2011**, *189*, 127−133.

(14) Deka, B. J.; Guo, J.; Jeong, S.; Kumar, M.; An, A. K. Emerging investigator series: control of membrane fouling by dissolved algal organic matter using pre-oxidation with coagulation as seawater pretreatment. *Environ. Sci. Water Res. Technol.* **2020**, *6*, 935−944.

(15) Rai, H. S.; Bhattacharyya, M. S.; Singh, J.; Bansal, T. K.; Vats, P.; Banerjee, U. C. Removal of dyes from the effluent of textile and dyestuff manufacturing industry: a review of emerging techniques with reference to biological treatment. *Crit. Rev. Environ. Sci. Technol.* **2005**, *35*, 219−238.

(16) Reddy, C. N.; Kumar, A. N.; Mohan, S. V. Metabolic Phasing of Anoxic-PDBR for High Rate Treatment of Azo Dye Wastewater. *J. Hazard. Mater.* **2018**, *343*, 49−58.

(17) Bai, Y. N.; Wang, X. N.; Zhang, F.; Wu, J.; Zhang, W.; Lu, Y. Z.; Fu, L.; Lau, T. C.; Zeng, R. J. High-rate anaerobic decolorization of methyl orange from synthetic azo dye wastewater in a methane-based hollow fiber membrane bioreactor. *J. Hazard. Mater.* **2020**, *388*, No. 121753.

(18) Rauf, M. A.; Meetani, M. A.; Khaleel, A.; Ahmed, A. Photocatalytic degradation of Methylene blue using a mixed catalyst and product analysis by LC/MS. *Chem. Eng. J.* **2010**, *157*, 373−378.

(19) Liu, Y. H.; Cao, X. H.; Hua, R.; Wang, Y. Q.; Liu, Y. T.; Pang, C.; Wang, Y. Selective adsorption of uranyl ion on ion-imprinted chitosan/PVA cross-linked hydrogel. *Hydrometallurgy* **2010**, *104*, 150−155.

(20) Ezugbe, E. O.; Rathilal, S. Membrane Technologies in Wastewater Treatment: A Review. *Membranes* **2020**, *10*, 89.

(21) Elzubair, A.; Uchôa, L. R.; da Silva, H. M. P. Production and characterization of graphene oxide/polymer support composite membranes for water desalination and purification. *Desalin. Water Treat.* **2024**, *317*, No. 100012.

(22) Jasim, H. K.; Al-Ridah, Z. A.; Naje, A. S. Graphene oxide−carbon nanotube composite membrane for enhanced removal of organic pollutants by forward osmosis. *Desalin. Water Treat.* **2024**, *318*, No. 100363.

(23) Khalil, A.; Maschietti, M.; Muff, J. Influence of graphene oxide additives on the NF separation of triazine-based H2S scavenging compounds using advanced membrane technology. *Chemosphere* **2024**, *360*, No. 142439.

(24) Wen, X.; Quintano, V.; Xie, Z.; Ren, X.; Stonehouse, G.; Bustamante, H.; Jin, X.; Joshi, R. Flake size-dependent water transport through graphene oxide membranes and rejection of geosmin (GSM) and 2-methylisoborneol (MIB) from drinking water. *Carbon* **2024**, *229*, No. 119543.

(25) Krishnamoorthi, R.; Butt, F. S.; Mazlan, N. A.; Chen, S.; Radacsi, N.; Yang, S.; Yoon, Y.; Huang, Y. Tuning the interlayer spacing of graphene oxide membrane via surfactant intercalation for ultrafast nanofiltration. *J. Membr. Sci.* **2024**, *706*, No. 122942.

(26) Mazlan, N. A.; Lewis, A.; Chen, Z.; Butt, F. S.; Han, J.; Radacsi, N.; Yang, S.; Huang, Y. Photocatalytic self-cleaning graphene oxide/ZnO hybrid membrane for ultrafast cyclic small organic molecule separation. *J. Membr. Sci.* **2024**, *697*, No. 122539.

(27) Geren, M. B. A.; Chen, G. Q.; Li, D.; Kentish, S. E. Equilibrium ion sorption in graphene oxide membranes. *J. Membr. Sci.* **2024**, *710*, No. 123155.

(28) Zhang, J.; Hu, F. T.; Liu, Q. Q.; Zhao, X.; Liu, S. Q. Application of heterogenous catalyst of tris(1,10)- phenanthroline iron(II) loaded on zeolite for the photoFenton degradation of methylene blue. *React. Kinet. Mech. Catal.* **2011**, *103*, 299−310.

(29) Aurellia, J. M.; Maulida, G.; Dzujah, D. U.; Syakir, N.; Fitrilawati. Effect of Stirring Time on Methylene Blue Adsorption onto Graphene Oxides. *Mater. Sci. Forum* **2021**, *1028*, 291−295.
(30) Maulida, G.; Aurellia, J. M.; Dzujah, D. U.; Syakir, N.; Fitrilawati. Study of Methylene Blue Adsorption onto Aminated Graphene Oxides at Varied Stirring Time. *Mater. Sci. Forum* **2021**, *1028*, 308−312.
(31) Joshi, J. R. K.; Alwarappan, S.; Yoshimura, M.; Sahajwalla, V.; Nishina, Y. Review: Graphene oxide: the new membrane material. *Appl. Mater. Today* **2015**, *1*, 1−12.
(32) Park, S.; Choi, K. S.; Lee, D.; Kim, D.; Lim, K. T.; Lee, K.-H.; Seonwoo, H.; Kim, J. Eggshell membrane: Review and impact on engineering. *Biosyst. Eng.* **2016**, *151*, 446−463.
(33) Mahmood, A. R.; Abdallah, I. Q.; Alheety, M. A.; Akbaş, H.; Karadağ, A. N, O-rich graphene oxide based eggshell membrane polymer: Preparation, characterization and its utility as nano sorbent for solid phase extraction of Pb (II) in various water samples. *AIP Conf. Proc.* **2019**, *2144*, No. 020003.
(34) Preda, N.; Costas, A.; Beregoi, M.; Apostol, N.; Kuncser, A.; Curutiu, C.; Iordache, F.; Enculescu, I. Functionalization of eggshell membranes with CuO−ZnO based p−n junctions for visible light induced antibacterial activity against *Escherichia coli*. *Sci. Rep.* **2020**, *10*, No. 20960.
(35) Lin, M. F.; Chang, P. Y.; Lee, C. H.; Wu, X. X.; Jeng, R. J.; Chen, C.-P. Biowaste Eggshell Membranes for Bio-triboelectric Nanogenerators and Smart Sensors. *ACS Omega* **2023**, *8*, 6699−6707.
(36) Maulida, G.; Fauziah, Y.; Bahtiar, A.; Syakir, N.; Fitrilawati. Eggshell-Graphene Oxide Layer as Membrane Filtration for Removal Methylene Blue in Waste Water. *J. Phys.: Conf. Ser.* **2022**, *2376*, No. 012002.
(37) Piry, A.; Heino, A.; Kühnl, W.; Grein, T.; Ripperger, S.; Kulozik, U. Effect of membrane length, membrane resistance, and filtration conditions on the fractionation of milk proteins by microfiltration. *J. Dairy Sci.* **2011**, *95*, 1590−1602.
(38) Nor, N. M.; Azmir, M. I. M.; Amri, N. Surface Chemistry Interaction of Graphene Oxide/Eggshell Adsorbent towards Fluoride Removal. *Adv. Sci. Technol.* **2023**, *127*, 65−73.
(39) Feng, C.; Xu, J.; Li, M.; Tang, Y.; Gao, C. Studies on a novel nanofiltration membrane prepared by cross-linking of polyethyleneimine on polyacrylonitrile substrate. *J. Membr. Sci.* **2014**, *451*, 103−110.
(40) Xu, W. L.; Fang, C.; Zhou, F.; Song, Z.; Liu, Q.; Qiao, R.; Yu, M. Self-Assembly: A Facile Way of Forming Ultrathin, High-Performance Graphene Oxide Membranes for Water Purification. *Nano Lett.* **2017**, *17*, 2928−2933.
(41) Januário, E. F. D.; Vidovix, T. B.; Beluci, N. C. L.; Paixão, R. M.; Silva, L.H.B.R.D.; Homem, N. C.; Bergamasco, R.; Vieira, A. M. S. Advanced graphene oxide-based membranes as a potential alternative for dyes removal: A review. *Sci. Total Environ.* **2021**, *789*, No. 147957.
(42) Hu, M.; Mi, B. Layer-by-layer assembly of graphene oxide membranes via electrostatic interaction. *J. Membr. Sci.* **2014**, *469*, 80−87.
(43) Zeng, H.; Yu, Z.; Shao, L.; Li, X.; Zhu, M.; Liu, Y.; Feng, X.; Zhu, X. A novel strategy for enhancing the performance of membranes for dyes separation: Embedding PAA@UiO-66-NH2 between graphene oxide sheets. *Chem. Eng. J.* **2021**, *403*, No. 126281.
(44) Jinnah, S. N. H. M. A.; Ali, U. F. M.; Gopinath, S. C. B.; Ibrahim, N.; Ahmad, R.; Zuki, F. M. Oil palm waste-derived reduced graphene oxide (rGO) for dynamic adsorption of dye in a fixed-bed system. *Desalin. Water Treat.* **2024**, *317*, No. 100019.
(45) Wu, S. C.; Hsu, H. C.; Hsu, S. K.; Chang, Y. C.; Ho, W. F. Synthesis of hydroxyapatite from eggshell powders through ball milling and heat treatment. *J. Asian Ceram. Soc.* **2016**, *4*, 85−90.
(46) Nakano, T.; Ikawa, N. I.; Ozimek, L. Chemical Composition of Chicken Eggshell and Shell Membranes. *Poult. Sci.* **2003**, *82*, 510−514.
(47) Draper, M. H.; Davidson, M. F.; Wyburn, G. M.; Johnston, H. S. The fine structure of the fibrous membrane forming region of the isthmus of the oviduct of gallus domesticus. *Exp. Physiol.* **1972**, *57*, 297−309.
(48) Du, J.; Hincke, M. T.; Rose-Martel, M.; et al. Identifying specific proteins involved in eggshell membrane formation using gene expression analysis and bioinformatics. *BMC Genomics* **2015**, *16*, 792.
(49) Fitrilawati; Fauziah, Y.; Maulida, G.; Syakir, N. Uji Filtrasi Model Polutan Methylen Blue Menggunakan Membran Kulit Telur. *J. Inovasi Fis.* **2022**, *6*, 81−89.
(50) Hung, W. S.; An, Q. F.; De Guzman, M.; Lin, H. Y.; Huang, S. H.; Liu, W. R.; Hu, C. C.; Lee, K. R.; Lai, J. Y. Pressure-assisted self-assembly technique for fabricating composite membranes consisting of highly ordered selective laminate layers of amphiphilic graphene oxide. *Carbon* **2014**, *68*, 670−677.
(51) Nan, Q.; Li, P.; Cao, B. Fabrication of positively charged nanofiltration membrane via the layer-by-layer assembly of graphene oxide and polyethylenimine for desalination. *Appl. Surf. Sci.* **2016**, *387*, 521−528.
(52) Ashfaq, M. Y.; Al-Ghouti, M. A.; Zouari, N. Investigating the effect of polymer-modified graphene oxide coating on RO membrane fouling. *J. Water Process Eng.* **2022**, *49*, 103164.

https://doi.org/10.1021/acsomega.4c05853
ACS Omega 2024, 9, 51052−51061